



Synthesis, crystal structure, and magnetic property of a cobalt(II) complex constructed from symmetrical 2-fluoroisonicotinate

Gui-Lin Wen, Ming-Rong Hua, Xiao-Ling Wang, Xian Liang, Dong Tian & Xing Zhao

To cite this article: Gui-Lin Wen, Ming-Rong Hua, Xiao-Ling Wang, Xian Liang, Dong Tian & Xing Zhao (2016) Synthesis, crystal structure, and magnetic property of a cobalt(II) complex constructed from symmetrical 2-fluoroisonicotinate, *Molecular Crystals and Liquid Crystals*, 631:1, 154-163, DOI: [10.1080/15421406.2016.1170277](https://doi.org/10.1080/15421406.2016.1170277)

To link to this article: <http://dx.doi.org/10.1080/15421406.2016.1170277>



Published online: 12 Jul 2016.



Submit your article to this journal [↗](#)



Article views: 24



View related articles [↗](#)



View Crossmark data [↗](#)

Synthesis, crystal structure, and magnetic property of a cobalt(II) complex constructed from symmetrical 2-fluoroisonicotinate

Gui-Lin Wen, Ming-Rong Hua, Xiao-Ling Wang, Xian Liang, Dong Tian, and Xing Zhao

School of Chemistry and Materials Engineering, Anhui Key Laboratory of Low Temperature Co-fired Materials, Huainan Normal University, Huainan, China

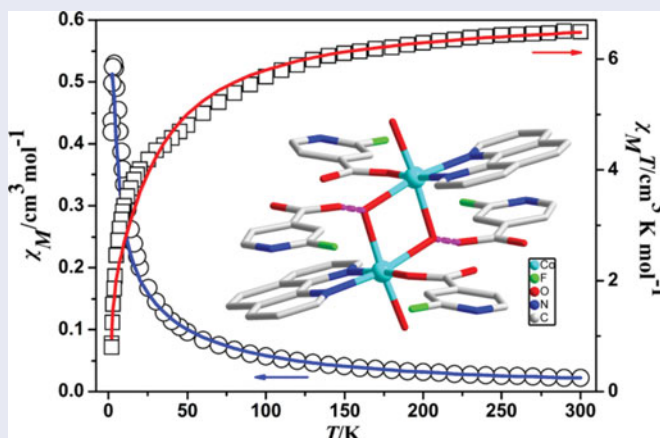
ABSTRACT

A new complex, $[\text{Co}_2(\text{OH})_2\text{L}_2(\text{phen})_2(\text{H}_2\text{O})_2] \cdot 2(\text{HL})$ (**1**) (HL = 2-fluoroisonicotinic acid, phen = 1,10-phenanthroline), has been synthesized using the slow-layered diffusion technique at room temperature. Single crystal X-ray analysis revealed that complex **1** is a dinuclearcobalt(II) complex connected by hydroxyl oxygen. The thermal stability was studied by thermogravimetric analysis (TGA). In addition, the variable-temperature magnetic property of the complex has been also discussed. The negative θ , J or $-E_2/k$ values can be indicative of an overall antiferromagnetic coupling in addition to single-ionspin-orbital coupling.

KEYWORDS

2-Fluoroisonicotinic acid;
cobalt(II) complex;
antiferromagnetic property

GRAPHICAL ABSTRACT



An interesting dinuclearcobalt(II) complex based on 2-fluoroisonicotinic acid were synthesized and structurally characterized. The two Co(II) centers are linked by $\mu_2\text{-OH}^-$ groups and there are uncoordinated HL molecules in the structure too. The thermal and the variable-temperature magnetic properties of the complex are also discussed. The negative θ , J or $-E_2/k$ values can be indicative of an overall antiferromagnetic coupling in addition to single-ionspin-orbital coupling.

Introduction

Metal coordination complexes are nowadays very popular topic in the fields of chemistry and materials research due to their novel architecture as well as potential applications as functional materials. [1,2] In particular, molecule-based magnetic materials (such as single molecule magnets (SMMs) and single chain magnets (SCMs)), which exhibit new magnetic phenomena or useful magnetic properties, have been actively investigated and become very attractive targets in crystal engineering [3–5]. The organic linkers play a crucial role in the exchange magnetic interactions among the neighboring magnetic carriers because magnetism is a cooperative phenomenon [6,7]. Aromatic carboxylate anions have been used frequently to synthesize magnetic materials because of their diverse binding capability and efficiency in transmitting magnetic coupling [8,9]. Metal-carboxylates (in particular those Co(II) carboxylates) have shown to be potential candidates to construct molecular magnets, exhibiting various bulk magnetic behaviors [9–13]. Moreover, the $\pi \cdots \pi$ interaction of rigid aromatic skeletons, mainly responsible for tuning magnetic interaction between the metal centers, may result in interesting physical properties [14]. The magnetism of dinuclear high-spin cobalt(II) complexes is a challenging area because the orbital angular momentum causes difficulties in the magnetic analysis [15–18]. On the other hand, although nicotinic acid and isonicotinic acid, as good sources of carboxylate ligands, have been widely applied to construct coordination compounds, fluorinated nicotinic acid and isonicotinic acid have not been studied in depth [19]. Only several 1D lanthanide coordination polymers based on 2-fluoroisonicotinic acid have been synthesized and characterized not long before [19]. As a continuation of this project, here we present the syntheses and crystal structure of a new complex containing this ligand, which is $[\text{Co}_2(\text{OH})_2\text{L}_2(\text{phen})_2(\text{H}_2\text{O})_2] \cdot 2(\text{HL})(\mathbf{1})$. Furthermore, the thermal behaviors and the variable-temperature magnetic properties of the complex are also discussed in details.

Experimental section

Materials and physical techniques

All reagents and solvents employed were commercially available and used as received without further purification. Elemental analyses (C, H, and N) were carried out in a Thermo Science Flash 2000 organic element analyzer. Infrared spectra on KBr pellets were recorded on Bruker EQUINOX-55 FT-IR spectrophotometer in the range of $4000 \sim 400 \text{ cm}^{-1}$. Thermal analyses were performed on a NETZSCH STA 449C microanalyzer with a heating rate of $10^\circ\text{C} \cdot \text{min}^{-1}$ under N_2 atmosphere. The powder X-ray diffraction (PXRD) patterns were measured using a Bruker D8 advance powder diffractometer at 40 kV and 40 mA for Cu- $K\alpha$ radiation ($\lambda = 1.5418 \text{ \AA}$), with a scan speed of 0.2 s per step and a step size of $0.02^\circ (2\theta)$. Magnetic data were obtained using a Quantum Design MPMS SQUID 7S magnetometer at an applied field of 1000 Oe using multicrystalline samples of **1** in the temperature range of 1.9–300 K. The magnetic susceptibilities were corrected using Pascal's constant and the diamagnetism of the holder.

Synthesis of $[\text{Co}_2(\text{OH})_2\text{L}_2(\text{phen})_2(\text{H}_2\text{O})_2] \cdot 2(\text{HL})(\mathbf{1})$

An aqueous solution (6 mL) of HL (0.2 mmol) (The pH was adjusted to about 7 with an aqueous solution of 1 M KOH) was mixed with an aqueous solution (3 mL) of $\text{Co}(\text{NO}_3)_2 \cdot 6\text{H}_2\text{O}$ (0.1 mmol) and the resulting solution was stirred for 15 min to mix well. Then in a glass tube

Table 1. Crystallographic data and structure refinement summary for **1**.

Complex	1
Formula	$C_{48}H_{36}Co_2F_4N_8O_{12}$
F_w	1110.71
Crystal system	Triclinic
Space group	$P\bar{1}$ (No. 2)
$a/\text{\AA}$	7.362(4)
$b/\text{\AA}$	11.757(6)
$c/\text{\AA}$	14.665(7)
$\alpha/^\circ$	103.761(7)
$\beta/^\circ$	100.982(7)
$\gamma/^\circ$	99.616(7)
$V/\text{\AA}^3$	1179.9(10)
Z	1
$D_{\text{calc}}/\text{g cm}^{-3}$	1.563
$F(000)$	566
Reflections collected / unique	16622 / 5833
R_{int}	0.0269
Completeness	99.8% ($\theta = 25.242$)
GOF on F^2	1.153
Final R indices [$I > 2\sigma(I)$]	$R_1 = 0.0419$, $wR_2 = 0.1317$
R indices(all data)	$R_1 = 0.0523$, $wR_2 = 0.1457$
Largest diff. peak and hole/e \AA^{-3}	1.003 and -0.681

a methanol solution (8 mL) of phen (0.1 mmol) was slowly and carefully layered with the above mentioned mixed solution using 2 ml of buffer solution (1 : 1 of water and CH_3OH) in between the two solutions. The tube was sealed and kept undisturbed at room temperature and after one week red block crystals were obtained from the junction of the layers. The crystals were separated and washed with CH_3OH and air-dried. Yield: 64% based on cobalt. Elemental analysis (%) for $C_{48}H_{36}Co_2F_4N_8O_{12}$, Calcd: C, 51.90; H, 3.27; N, 10.09. Found: C, 52.02; H, 3.16; N, 10.18. IR (KBr pellet, cm^{-1}): 3409w, 3047w, 1603s, 1565s, 1403vs, 1379s, 1284w, 1231m, 1150w, 1102w, 1088w, 936w, 893w, 855m, 774m, 726m, 678m, 573w, 445w.

Single crystal structure determination

Crystallographic data for **1** were collected at room temperature with a Bruker Apex II Image Plate single-crystal diffractometer with graphite-monochromated Mo- $K\alpha$ radiation source ($\lambda = 0.71073 \text{ \AA}$) operating at 50 kV and 30 mA in ω scan mode for **1**. A multi-scan absorption correction was applied with the use of SADABS. The structures were solved by direct methods and refined by full-matrix least-squares refinements based on F^2 with the SHELXTL program[20]. All nonhydrogen atoms were refined anisotropically with the hydrogen atoms added to their geometrically ideal positions and refined isotropically. The detailed crystallographic data and structure refinement parameters for **1** are summarized in Table 1 and selected bond lengths and angles are given in Table 2. CCDC: 1056344 contains the supplementary crystallographic data for complex **1**. Possible hydrogen bond geometries of **1** are shown in Table 3.

Results and discussion

Syntheses

The mixing simply in traditional aqueous reactions or hydrothermal treatment of the all starting materials produces powdered precipitation or irregular crystals with poor quality.

Table 2. Selected bond lengths [Å] and angles [°] for complex 1.

Co1-O5	2.0632(19)	Co1-N4	2.1373(19)
Co1-O2	2.0775(17)	Co1-O6#1	2.1390(17)
Co1-N3	2.103(2)	Co1-O6	2.1797(18)
O5-Co1-O2	90.33(7)	O5-Co1-O6#1	95.54(7)
O5-Co1-N3	95.32(8)	O2-Co1-O6#1	89.71(6)
O2-Co1-N3	92.92(7)	N3-Co1-O6#1	168.81(6)
O5-Co1-N4	88.67(7)	N4-Co1-O6#1	98.80(7)
O2-Co1-N4	171.48(6)	O5-Co1-O6	174.82(6)
N3-Co1-N4	78.76(7)	O2-Co1-O6	89.83(6)
N3-Co1-O6	89.84(7)	O6#1-Co1-O6	79.29(6)
N4-Co1-O6	91.93(6)	Co1#1-O6-Co1	100.71(6)

Symmetry codes: #1 $-x, -y+2, -z+1$.

Therefore, liquid diffusion method was used to grow crystals, which methanol solution of phen and aqueous solution of HL/inorganic salts were placed on the top and bottom of test tube. Fortunately, several days later, a lot of red block crystal products with high quality were obtained on the interface between the water phase and the methanol phase. PXRD analyses reveal only one kind of substance, namely the title product, was gained, which suggests the chemical stability of the crystal structures in the given conditions. Furthermore, we designed an experiment with a series of liquid diffusion reactions containing some influence factors such as pH value, solvent dosage and metal-ligand stoichiometric ratios in the attempt to disclose the crucial factors from it. The results show that the reaction is sensitive to the pH value of synthesis system, and the crystals grew well in the neutral range. Differently, solvent dosage and varying stoichiometric ratios of used precursors have scarcely any influence on the crystalline state of the products.

Description of crystal structures

Single crystal X-ray analysis revealed **1** crystallizes in the triclinic $P\bar{1}$ space group. The asymmetric unit consists of one crystallographically independent Co(II) cation, one deprotonated L^- anion, one μ_2 -OH $^-$, a phen ligand, a coordinated water molecule, and one uncoordinated HL (Fig. 1). Each Co center is octahedrally coordinated by two O atoms from two μ_2 -OH $^-$ groups (O6 and O6A) with the Co–O distance of 2.1797(18) and 2.1390(17) Å, a carboxylic O atom (O2) from L^- ligand (Co–O 2.0775(17) Å), two N atoms of phen molecule (Co–N2.103(2) and 2.1373(19) Å) and one water molecule (Co–O 2.0632(19) Å). Two adjacent Co(II) centers are doubly linked by two μ_2 -OH $^-$ groups with the Co...Co distance of 3.3258(14) Å and the Co–O–Co angle of 100.71(6)°. Each carboxyl group of L^- adopts the

Table 3. Selected hydrogen-bond geometry [Å°] for complex 1.

D–H...A	D–H	H...A	D...A	D–H...A
O3–H3A...O6#2	0.82	1.82	2.537(2)	146
O5–H5B...O1#4	0.96	1.96	2.738(3)	136.4
O5–H5A...O4	0.96	1.73	2.636(3)	156.7
O6–H6A...O1#1	0.802(18)	1.92(2)	2.665(2)	153(3)
C13–H13...O2	0.93	2.66	3.188(3)	117
C22–H22...O3#4	0.93	2.46	3.375(3)	166.8
C5–H5...F3#3	0.93	2.58	3.327(5)	137.7
C14–H14...N2#6	0.93	2.58	3.464(4)	159.9
C21–H21...N1#5	0.93	2.67	3.567(4)	162.7

Symmetry codes: #1 $-x, -y+2, -z+1$; #2 $x+1, y, z$; #3 $-x+1, -y+2, -z$; #4 $-x+1, -y+2, -z+1$; #5 $x, y, z+1$; #6 $-x, -y+1, -z$.

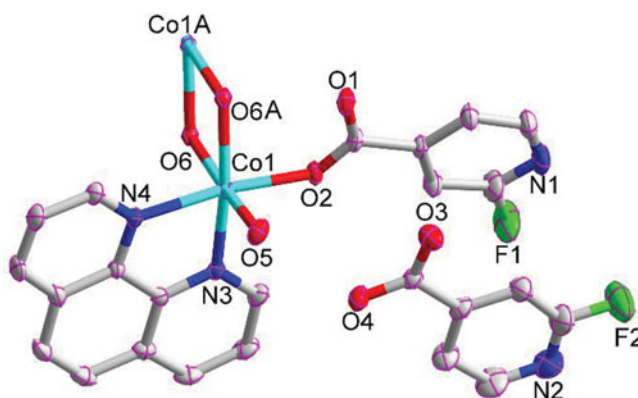


Figure 1. A view of the asymmetric unit of **1** and the local coordination of the Co(II) cation. Displacement ellipsoids are drawn at the 30% probability level. [Symmetry codes: A $-x$, $-y+2$, $-z+1$].

monodentate binding mode, while the pyridyl group of L^- in **1** is not involved in the coordination.

As shown in Fig. 2, the adjacent Co_2 dimers link each other through double hydrogen bonds between uncoordinated carboxylate oxygens (O1) and the coordinated aqua molecules (O5) to give a 1D ladder-like supramolecular chain along the a axis with the $O\cdots O$ distance of 2.738(3) Å. Meanwhile, the uncoordinated HL molecules are hydrogen bonded to the chain through $O-H\cdots O$ hydrogen bonds between carboxylate O atoms and water molecules/hydroxyl groups.

Furthermore, the adjacent supramolecular ladder-like chains are extended via the intermolecular $C-H\cdots N$ interactions (between the pyridyl N atoms of L^- and phen rings) along the c axis with the $C\cdots N$ distance of 3.567(4) Å and the face-to-face $\pi\cdots\pi$ stacking between phen rings along the a axis with the interplanar distance of 3.455(7) and 3.346(4) Å into a three-dimensional supramolecular framework (Fig. 3). The uncoordinated HL molecules are further consolidated in the structure by $C-H\cdots N/F$ interactions.

PXRD and thermogravimetric analysis (TGA)

The powder X-ray diffraction (PXRD) pattern of the as-synthesized sample matches the simulation based on the single-crystal diffraction data, which indicates the phase purity of the

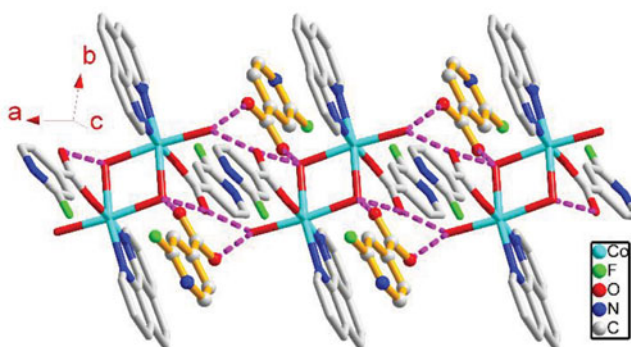


Figure 2. The 1D ladder-like supramolecular chain along the a axis (pink dashed lines represent the hydrogen bonds). H atoms have been omitted for clarity.

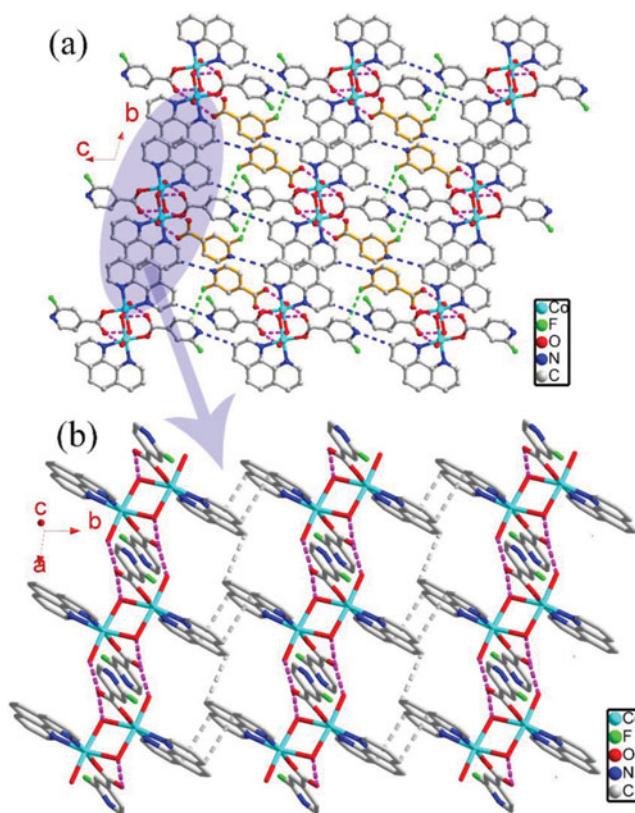


Figure 3. (a) The three-dimensional supramolecular framework of **1**. (b) the face-to-face $\pi \cdots \pi$ stacking between phen rings along the *a* axis. H atoms and some uncoordinated HL molecules have been omitted for clarity.

product (Fig. 4). TGA of complex **1** was performed in the temperature range of 25–850°C under a nitrogen atmosphere. The TG curve in Fig. 5 shows no obvious weight loss from 25 to 85°C. An initial weight loss of ~6.0% is observed at around 85–115°C indicating the loss of the coordinated water and the OH[−] in a single step (calcd. 6.3%). The dehydrated framework of **1** is thermally stable up to 245°C, and then a large weight loss of about 31.5% is observed at around 245–370°C, which is consistent with the loss of the phen ligand (calcd. 32.4%). After about 525°C, the weight loss corresponds to the release of organic ligands accompanying by an ulterior thermal decomposition.

The variable-temperature magnetic susceptibility data of complex **1** was collected in the temperature range of 1.8–300 K under a field of 1000 Oe. As shown in Fig. 6, the room temperature $\chi_M T$ value is 6.48 cm³ K mol^{−1}, which is significantly larger than the expected value 3.75 cm³ K mol^{−1} for two spin-only Co(II) ($S = 3/2$) ions with $g = 2$, indicating the important orbital contribution arising from the high-spin octahedral Co(II) centers [21–23]. With a decrease of the temperature, the $\chi_M T$ value decreases slowly and then more rapidly at low temperature, reaching 0.42 cm³ K mol^{−1} at 2.0 K. Above 50 K, the variation of $1/\chi_M$ with temperature follows the Curie–Weiss equation [$1/\chi_M = (T - \Theta)/C$] with $\Theta = -19.95$ K and $C = 6.90$ cm³ K mol^{−1} and $R = \Sigma[(1/\chi_M)_{\text{obs}} - (1/\chi_M)_{\text{calc}}]^2 / \Sigma[(1/\chi_M)_{\text{obs}}]^2 = 4.28 \times 10^{-5}$. The decrease of the $\chi_M T$ value or the negative Θ value can be induced by antiferromagnetic coupling interactions within and between dimeric units as well as strong spin-orbit coupling [24].

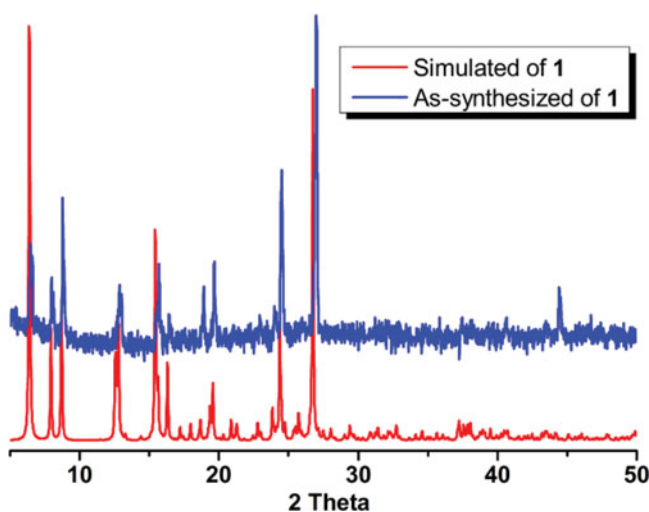


Figure 4. The powder X-ray diffraction (PXRD) patterns for **1**.

Magnetic properties

The antiferromagnetic behavior of **1** can be also understood on the basis of its structural feature: the exchange pathway between two adjacent Co(II) ions consists of two μ_2 -OH[−] groups with the Co–O–Co angle of 100.71(6)°, which surpasses the range for ferromagnetic exchange pathways (less than 97°) [7,13,25]. Although the magnetic analysis for the CoII complexes is rather difficult due to its spin–orbit coupling, the simple phenomenological equation is usually used to analyze the magnetic interactions between the Co(II) ions: $\chi_M T = A \exp(E_1/kT) + B \exp(E_2/kT)$, where $A + B$ equals the Curie constant, and E_1 and E_2 stand for the energies corresponding to the spin–orbit coupling and antiferromagnetic exchange interaction, respectively [22,26,27]. The best fitting results are $A + B = 6.89 \text{ cm}^3 \text{ K mol}^{-1}$, $E_1/k = 36.0 \text{ K}$, and $-E_2/k = -1.7 \text{ K}$ ($R = \sum[(\chi_M T)_{\text{obs}} - (\chi_M T)_{\text{calc}}]^2 / \sum[(\chi_M T)_{\text{obs}}]^2 = 8.02 \times 10^{-5}$). The obtained value of $A + B$ is very close to that from the Curie–Weiss law equation ($6.90 \text{ cm}^3 \text{ K mol}^{-1}$), and the obtained value of E_1/k has no significant difference from those

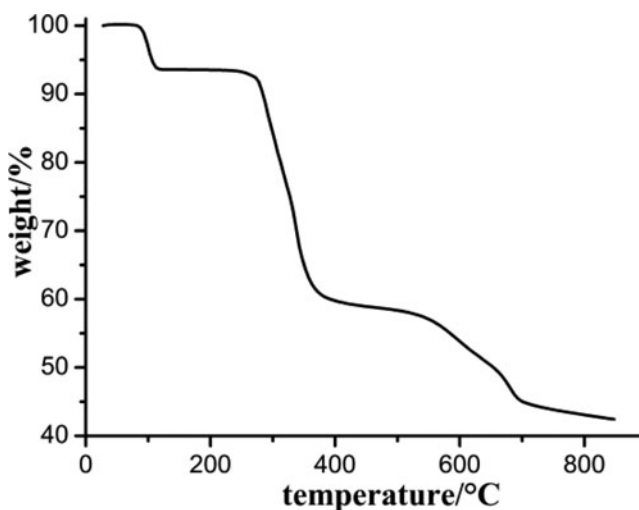


Figure 5. The TGA curve for **1** under a nitrogen atmosphere.

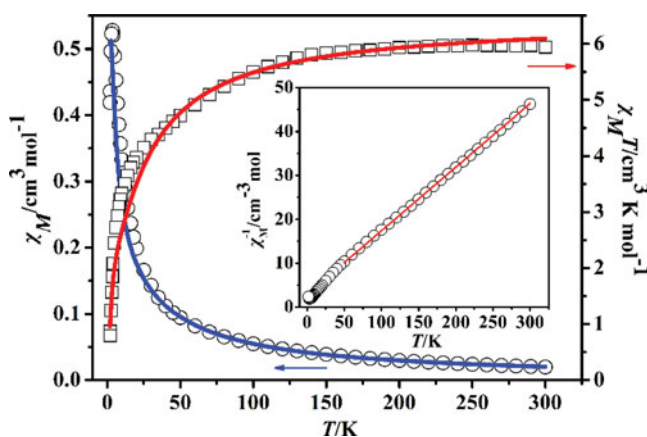


Figure 6. Plot of the χ_M vs. T , $\chi_M T$ vs. T , and $1/\chi_M$ vs. T for **1**. The solid lines correspond to the best fit according to the phenomenological equation.

given in the literature [27]. The negative value of $-E_2/k$ (-1.7 K) also indicates the dominant antiferromagnetic coupling between Co(II) ions analyzed from the structure of dimeric unit. Considering that complex **1** is a dinuclear cobalt(II) complex connected by hydroxyl oxygen, the magnetic susceptibility data above 50 K were thus approximately analyzed by an isotropic dimer mode of spin $S = 3/2$, as shown below [2,23,28]:

$$\chi_{\text{dim}} = \frac{2Ng^2\beta^2}{kT} \frac{e^{5x} + 5e^{3x} + 14}{e^{6x} + 3e^{5x} + 5e^{3x} + 7} \quad (1)$$

$$\chi_M = \frac{\chi_{\text{dim}}}{1 - (zJ'/Ng^2\beta^2)\chi_{\text{dim}}} \quad (2)$$

Where $x = -2J/kT$, J and zJ' represent intradimer and interdimer magnetic exchange interaction, respectively. The N , β , g , k , and T terms have their usual meanings. The least-squares analysis of magnetic susceptibilities data led to $J = -3.90$ cm $^{-1}$, $g = 2.71$, $zJ' = -0.60$ cm $^{-1}$, $R = 3.50 \times 10^{-5}$. The larger value of the g parameter may be due to significant orbital effect [29]. The negative J value also supports the presence of antiferromagnetic interactions in complex **1**. It is noticed that the zJ' component supports the weak interdimer antiferromagnetic contacts through abundant hydrogen bonds and $\pi \cdots \pi$ interaction.

Conclusions

In summary, a new dimer cobalt(II) complex based on asymmetrical 2-fluoroisonicotate was synthesized and structurally characterized. The two Co(II) centers are linked by μ_2 -OH $^-$ groups and there are uncoordinated HL molecules in the structure. The variable temperature magnetic property of the complex was investigated. Dominant antiferromagnetic interactions are found in it due to the large Co–O–Co angle. Further work is in progress to explore new materials based on the ligand and other related ligands which may show interesting physical or chemical properties.

Supporting information

The supplementary crystallographic data (CCDC: 1056344) for this paper can be obtained free of charge from the Cambridge Crystallographic Data Centre via www.ccdc.cam.ac.uk/data_request/cif.

Acknowledgments

This work was financially supported by the National Natural Science Foundation of China (Grant No. 21301062), Anhui Provincial Natural Science Foundation (Grant Nos. 1308085QB36 and 1408085QB23), Anhui Provincial Support Plan for Outstanding Young Talent in Colleges and Universities, National College Students' Innovative Entrepreneurial Training Program of Local colleges and universities (Grant No. 201410381018), and College students' extracurricular science and technology innovation fund of Huainan Normal University (Grant No. 2015XS110).

References

- [1] Sakata, Y., Furukawa, S., Kondo, M., Hirai, K., Horike, N., Takashima, Y., Uehara, H., Louvain, N., Meilikhov, M., Tsuruoka, T., Isoda, S., Kosaka, W., Sakata, O. & Kitagawa, S. (2013). *Science*, 339, 193–196.
- [2] Yan, W. H., Bao, S. S., Huang, J., Ren, M., Sheng, X. L., Cai, Z. S., Lu, C. S., Meng, Q. J. & Zheng, L. M. (2013). *Dalton Trans.*, 42, 8241–82418.
- [3] Clemente-Juan, J. M., Coronado, E., MínguezEspallargas, G., Adams, H. & Brammer, L. (2010). *Cryst. Eng. Comm.*, 12, 2339–2342.
- [4] Sheikh, J. A., Adhikary, A., Jena, H. S., Biswas, S., & Konar, S. (2014). *Inorg. Chem.*, 53, 1606–1613.
- [5] Zheng, Y.-Z., Zhou, G.-J., Zheng, Z., & Winpenny, R. E. P. (2014). *Chem. Soc. Rev.*, 43, 1462–1475.
- [6] Zou, G.-D., He, Z.-Z., Tian, C.-B., Zhou, L.-J., Feng, M.-L., Zhang, X.-D., & Huang, X.-Y. (2014). *Cryst. Growth & Des.*, 14, 4430–4438.
- [7] Chen, D. M., Ma, X. Z., Zhang, X. J., Xu, N., & Cheng, P. (2015). *Inorg. Chem.*, 54, 2976–2982.
- [8] Luo, F., Che, Y.-X., & Zheng, J.-M. (2009). *Cryst. Growth & Des.*, 9, 1066–1071.
- [9] Lama, P., Mrozinski, J., & Bharadwaj, P. K. (2012). *Cryst. Growth & Des.*, 12, 3158–3168.
- [10] Chu, Q., Su, Z., Fan, J., Okamura, T., Lv, G.-C., Liu, G.-X., Sun, W.-Y., & Ueyama, N. (2011). *Cryst. Growth & Des.*, 11, 3885–3894.
- [11] Li, J., Li, B., Huang, P., Shi, H. Y., Huang, R. B., Zheng, L. S., & Tao, J. (2013). *Inorg. Chem.*, 52, 11573–11579.
- [12] Huang, F.-P., Tian, J.-L., Gu, W., Liu, X., Yan, S.-P., Liao, D.-Z., & Cheng, P. (2010). *Cryst. Growth & Des.*, 10, 1145–1154.
- [13] Bernini, M. C., de Paz, J.R., Snejkó, N., Sáez-Puche, R., Gutierrez-Puebla, E., & Monge, M.Á. (2014). *Inorg. Chem.*, 53, 12885–12895.
- [14] Bhatt, P., Thakur, N., Meena, S. S., Mukadam, M. D., & Yusuf, S. M. (2013). *J. Mater. Chem. C*, 1, 6637–6652.
- [15] Hossain, M. J., Yamasaki, M., Mikuriya, M., Kuribayashi, A., & Sakiyama, H. (2002). *Inorg. Chem.*, 41, 4058–4062.
- [16] Jing, X. H., Yi, X. C., Gao, E. Q., & Blatov, V. A. (2012). *Dalton Trans.*, 41, 14316–14328.
- [17] Wei, Y., Yu, Y., Sa, R., Li, Q., & Wu, K. (2009). *Cryst. Eng. Comm.*, 11, 1054–1060.
- [18] Ma, T., Li, M.-X., Wang, Z.-X., Zhang, J.-C., Shao, M., & He, X. (2014). *Cryst. Growth & Des.*, 14, 4155–4165.
- [19] Wang, X.-M., Wu, W.-P., Jiang, Y.-H., Yang, G.-P., & Xi, Z.-P. (2014). *Chin. J. Inorg. Chem.*, 30, 192–203.
- [20] Sheldrick G. M. (1997). *SHELXL-97/2013, program for the refinement of the crystal structures*. University of Göttingen: Germany.
- [21] Ren, C., Hou, L., Liu, B., Yang, G.-P., Wang, Y.-Y., & Shi, Q.-Z. (2011). *Dalton Trans.*, 40, 793–804.
- [22] Niu, C.-Y., Zheng, X.-F., Wan, X.-S., & Kou, C.-H. (2011). *Cryst. Growth & Des.*, 11, 2874–2888.
- [23] Ma, L. F., Wang, L. Y., Wang, Y. Y., Batten, S. R., & Wang, J. G. (2009). *Inorg. Chem.*, 48, 915–924.
- [24] Chen, Q., Zhou, Y.-L., & Zeng, M.-H. (2009). *J. Mole. Struct.*, 932, 55–60.

- [25] Liu, J. Q., Liu, B., Wang, Y. Y., Liu, P., Yang, G. P., Liu, R. T., Shi, Q. Z., & Batten, S. R. (2010). *Inorg. Chem.*, 49, 10422–10426.
- [26] Sen, R., Mal, D., Lopes, A. M., Brandao, P., Araujo, J. P., & Lin, Z. (2013). *Dalton Trans.*, 42, 14836–14843.
- [27] Cui, S.-X., Zhao, Y.-L., Zhang, J.-P., & Liu, Q. (2009). *J. Mole. Struct.*, 927, 21–26.
- [28] Ma, L.-F., Wang, L.-Y., Lu, D.-H., Batten, S. R., & Wang, J.-G. (2009). *Cryst. Growth & Des.*, 9, 1741–1749.
- [29] Bhattacharya, S., Goswami, A., Gole, B., Ganguly, S., Bala, S., Sengupta, S., Khanra, S., & Mondal, R. (2014). *Cryst. Growth & Des.*, 14, 2853–2865.